

# AERONOMIC PROBLEMS OF MOLECULAR OXYGEN PHOTODISSOCIATION—II. THEORETICAL ABSORPTION CROSS-SECTIONS OF THE SCHUMANN–RUNGE BANDS AT 79 K

MARCEL NICOLET,\* STANISLAS CIESLIK† and ROBERT KENNES

Institut d'Aéronomie Spatiale de Belgique, 3 Avenue Circulaire, B-1180 Brussels, Belgium

(Received 22 April 1988)

**Abstract**—Theoretical spectra corresponding to the domain of the rotation lines of the 2–0 to 12–0 bands of the  $B^3\Sigma_u^- - X^3\Sigma_g^-$  Schumann–Runge system of  $O_2$  at 79 K are presented in graphical format. Calculated absorption cross-sections are compared with recent laboratory measurements made at the same temperature. The calculations were based on previous theoretical determinations at 300 K established after a comparison with results of laboratory measurements made at the same temperature. Such an analysis in which the band oscillator strengths are associated with averaged linewidths of the rotation lines for each band and with their underlying continuum, gives consistent values for the various spectroscopic parameters of the  $O_2$  Schumann–Runge bands.

## 1. INTRODUCTION

In a recent publication (Nicolet *et al.*, 1987), a theoretical determination of the rotational structure and absorption cross-sections of the  $O_2$  Schumann–Runge bands (see Table 1) was made at 300 K. This detailed analysis was based on the experimental results obtained by the Harvard-Smithsonian Group on the photodissociation absorption cross-sections at high resolution in the spectral region corresponding to the  $v' = 1$ –12 bands (Yoshino *et al.*, 1983).

After the first detailed analyses such as the wavelength assignments, for  $v' \geq 12$ , of Brix and Herzberg (1954) and, for  $v' \leq 13$ , of Ackerman and Biaumé (1970) and Biaumé (1972), extensive wavenumber measurements of the rotation lines of the  $O_2$  Schumann–Runge absorption bands were provided by Yoshino *et al.* (1984). These sets of data are also the most accurate and most complete since the cross-sections are absolute, the linewidths being in excess of the instrument resolution for the various bands studied.

Recent rotational constants (Table 2) of the upper electronic state of the Schumann–Runge system have also been published by Cheung *et al.* (1986). These

constants make it possible to calculate the wavenumbers of the rotation lines. The same spectroscopic constants have been also determined by Lewis *et al.* (1986a,b) from the wavenumber measurements of Yoshino *et al.* (1984).

The adopted band oscillator strengths of the ( $v'$ , 0) and ( $v'$ , 1) bands were based on the various results of Yoshino *et al.* (1983), of Cheung *et al.* (1986), and of Lewis *et al.* (1986a).

The mean predissociation linewidths were determined after a detailed comparison between calculated absorption cross-sections and the experimental results published by Yoshino *et al.* (1983) in the spectral region corresponding to the  $v' = 1$ –12 bands. However, the absorption cross-sections throughout this region may depend also on the underlying continuum corresponding near  $50,000 \text{ cm}^{-1}$  to the  $O_2$  Herzberg continuum (see Nicolet and Kennes, 1986, 1988a). At wavenumbers greater than  $55,000 \text{ cm}^{-1}$ , the  $O_2$  Schumann–Runge continuum (see Lewis *et al.*, 1985a,b) plays a role related to the temperature.

The recent extensive determination by Yoshino *et al.* (1987) of the experimental structure of the 2–0 to 12–0 bands at 79 K provides a direct test for the theoretical determination which must be used for aeronomic purposes (temperatures generally between 170 and 270 K). In the present paper experimental data and theoretical results at 79 K are compared to provide an improved understanding of the absorption structure in the predissociation region of the  $O_2$  Schumann–Runge system.

\*Also with: Communications and Space Sciences Laboratory, Penn State University, University Park, PA 16802, U.S.A.

†Now at: Commission of the European Communities, ISFRA Establishment, Italy, Chemistry Division, Air Pollution Sector.

TABLE 1. ADOPTED SPECTRAL INTERVALS FOR THE SCHUMANN-RUNGE BANDS OF O<sub>2</sub>

Band	Wavenumber (cm <sup>-1</sup> )	Mean	$\Delta\nu$	Wavelength (nm)	Mean	$\Delta\lambda$
0-0	49000-49500	49250	500	204.08-202.02	203.04	2.06
1-0	49500-50050	49777	550	202.02-199.80	200.90	2.22
2-0	50050-50715	50382	665	199.80-197.18	198.48	2.62
3-0	50715-51355	51035	640	197.18-194.72	195.94	2.46
4-0	51355-51975	51665	620	194.72-192.40	193.55	2.32
5-0	51975-52565	52270	590	192.40-190.24	191.31	2.16
6-0	52565-53130	52847	565	190.24-188.22	189.22	2.02
7-0	53130-53660	53395	530	188.22-186.36	187.28	1.86
8-0	53660-54160	53910	500	186.36-184.64	185.49	1.72
9-0	54160-54625	54392	465	184.64-183.07	183.85	1.57
10-0	54625-55055	54840	430	183.07-181.64	182.35	1.43
11-0	55055-55440	55247	385	181.64-180.37	181.00	1.27
12-0	55440-55790	55615	350	180.37-179.14	179.80	1.13
13-0	55790-56090	55940	300	179.24-178.28	178.76	0.96
14-0	56090-56345	56217	255	178.28-177.48	177.88	0.80
15-0	56345-56550	56447	205	177.48-176.83	177.16	0.65
16-0	56550-56725	56637	175	176.83-176.29	176.56	0.57
17-0	56725-56855	56790	130	176.29-175.89	176.09	0.40
18-0	56855-56960	56907	105	175.89-175.56	175.72	0.33
19-0	56960-57035	56997	75	175.56-175.33	175.45	0.23

## 2. THE BAND OSCILLATOR STRENGTHS

The Schumann-Runge bands, analyzed many times, have generated several determinations of their mean oscillator strengths. The values adopted here (Table 3) are based mainly on the recent results of the Cambridge and Canberra groups to generate a consistent set of data (Yoshino *et al.*, 1983; Cheung *et al.*, 1984; Yoshino *et al.*, 1987; Lewis *et al.*, 1986a,b) and also on the analysis of Allison *et al.* (1971). Since it is practically impossible to introduce an exact oscillator strength adapted to all circumstances, mean values have been adopted for each vibrational level. The uncertainties should be generally less than 5% but could reach perhaps 5-10% for two or three bands. In any case, the values given in Table 3 must be considered as averaged band oscillator strengths to be adopted in order to determine the effective linewidths of the rotational lines of bands corresponding to the various vibrational levels from  $v' = 0$  to  $v' = 19$ .

## 3. ROTATIONAL PREDISSOCIATION LINEWIDTHS

The measured high resolution absorption cross-sections of the Schumann-Runge bands by Yoshino *et al.* (1983) between 201 and 179 nm have been adopted to determine the effective rotational linewidths. Even when experimental results exhibited systematic variations with rotational levels (Lewis *et al.*, 1986a,b), an equivalent band linewidth was adjusted to fit the experimental absolute cross-sections after the introduction of the effect of an underlying continuum.

The Herzberg continuum plays an important role in the determination of the absorption cross-sections of the first Schumann-Runge bands. The Schumann-Runge continuum is subject to a variation related to the population of the rotational and vibrational levels in the spectral range of the last bands near the normal continuum limit.

The best-fit model calculated values of the O<sub>2</sub> absorption cross-sections with the experimental

TABLE 2. ADOPTED SPECTROSCOPIC CONSTANTS FOR THE UPPER STATE OF THE SCHUMANN-RUNGE BANDS OF O<sub>2</sub> TO COMPUTE LINE POSITIONS

Band	$\nu_0$ (cm <sup>-1</sup> )	B <sub>v</sub>	D <sub>v</sub>	$\lambda_v$	$\gamma_v$
0-0	49357.96	0.8132	4.50 x 10 <sup>-6</sup>	1.69	- 2.80.x.10 <sup>-2</sup>
1-0	50045.53	0.7993	4.20	1.70	- 2.60
2-0	50710.68	0.7860	5.80	1.69	- 2.90
3-0	51351.94	0.7705	5.20	1.70	- 2.60
4-0	51969.36	0.7550	5.97	1.81	- 3.00
5-0	52560.94	0.7377	5.80	1.75	- 2.20
6-0	53122.65	0.7187	5.00	1.79	- 2.10
7-0	53655.95	0.7010	8.60	1.82	- 2.10
8-0	54156.22	0.6770	6.70	1.91	- 2.30
9-0	54622.50	0.6514	6.30	2.04	- 2.10
10-0	55051.16	0.6263	9.90	2.10	- 4.10
11-0	55439.23	0.5956	9.40	2.17	- 3.80
12-0	55784.58	0.5626	1.37 x 10 <sup>-5</sup>	2.37	- 5.40
13-0	56085.44	0.5242	1.63	2.51	- 8.40
14-0	56340.42	0.4832	2.09	2.81	- 1.16 x 10 <sup>-1</sup>
15-0	56550.62	0.4391	2.54	3.30	- 1.64
16-0	56719.62	0.3934	3.08	4.11	- 2.41
17-0	56852.45	0.3457	3.34	5.18	- 3.48
18-0	56951.60	0.2872	5.50	6.51	- 4.94
19-0	57025.80	0.2649	6.00	7.63	- 6.04

$\nu_0$  = band origin =  $T + \frac{2}{3} \lambda - \gamma$  as given by Cheung et al. (1986)

B<sub>v</sub> and D<sub>v</sub> = rotational constants for vibrational levels

$\lambda_v$  and  $\gamma_v$  splitting constants for vibrational levels.

For 18-0 and 19-0, see Fang, Wofsy and Dalgarno (1974).

measurements have been used to determine the rotational linewidths adapted to each band. The adopted mean rotational linewidths are given in Table 4. The computation was made at each 0.1 cm<sup>-1</sup> with a contributing spectral range of 500 cm<sup>-1</sup> for a Voigt profile. Since realistic high resolution synthetic spectra require line centers to be located to within about 0.1 cm<sup>-1</sup>, the wavenumbers obtained at each 0.1 cm<sup>-1</sup> between 49,000 and 57,000 cm<sup>-1</sup> give the possibility of determining the detailed structure of the whole spectrum and of studying the effect of temperature. In addition, the relative role of the underlying con-

tinua with their related accuracy can be investigated as a function of temperature and wavelength.

#### 4. THE O<sub>2</sub> HERZBERG CONTINUUM

The absorption cross-sections of the O<sub>2</sub> Herzberg continuum at wavelengths greater than 200 nm used before 1980 must now be replaced by experimental and observational results obtained recently (1984-1986). An analysis made by Nicolet and Kennes (1986, 1988) leads to the adoption of an empirical formula for the absorption cross-section,

TABLE 3. ADOPTED MEAN ABSORPTION OSCILLATOR STRENGTHS  $f_{v'v''}$  FOR THE SCHUMANN-RUNGE BANDS OF O<sub>2</sub> DEDUCED FROM ABSORPTION SPECTRA

$v'$	$f_{0v'}$	$f_{1v'}$
0	$2.8 \times 10^{-10}$	$7.6 \times 10^{-9}$
1	$3.0 \times 10^{-9}$	$8.2 \times 10^{-8}$
2	$1.9 \times 10^{-8}$	$4.6 \times 10^{-7}$
3	$8.2 \times 10^{-8}$	$1.8 \times 10^{-6}$
4	$2.7 \times 10^{-7}$	$5.0 \times 10^{-6}$
5	$7.4 \times 10^{-7}$	$1.3 \times 10^{-5}$
6	$1.6 \times 10^{-6}$	$2.7 \times 10^{-5}$
7	$3.4 \times 10^{-6}$	$5.0 \times 10^{-5}$
8	$6.2 \times 10^{-6}$	$8.6 \times 10^{-5}$
9	$1.0 \times 10^{-5}$	$1.2 \times 10^{-4}$
10	$1.5 \times 10^{-5}$	$1.7 \times 10^{-4}$
11	$1.9 \times 10^{-5}$	$2.1 \times 10^{-4}$
12	$2.4 \times 10^{-5}$	$2.6 \times 10^{-4}$
13	$2.7 \times 10^{-5}$	$2.6 \times 10^{-4}$
14	$2.8 \times 10^{-5}$	$2.9 \times 10^{-4}$
15	$2.7 \times 10^{-5}$	$2.7 \times 10^{-4}$
16	$2.6 \times 10^{-5}$	$2.0 \times 10^{-4}$
17	$2.2 \times 10^{-5}$	$1.6 \times 10^{-4}$
18	$1.7 \times 10^{-5}$	$1.3 \times 10^{-4}$
19	$1.3 \times 10^{-5}$	$1.6 \times 10^{-4}$

$$\sigma_{\text{HER}}(\text{O}_2) \text{ cm}^2,$$

$$\sigma_{\text{HER}}(\text{O}_2) = 7.5 \times 10^{-24} (v/5 \times 10^4) \times \exp \{ -50 [\ln (v/(5 \times 10^4))]^2 \} \text{ cm}^{-1}.$$

Although the available sets of Herzberg continuum cross-sections derived from laboratory measurements seem to reach an acceptable agreement with their experimental accuracy at wavelengths greater than 200 nm, the errors of the experimental or theoretical determinations prevent an exact extrapolation for the Herzberg continuum underlying the Schumann-Runge bands between 190 and 200 nm. Nevertheless, the stratospheric determinations are not in disagreement with the values deduced from the formula that we have adopted.

Since our final determinations of the oxygen transmittance and of the photodissociation rate constants

are given for spectral intervals of 500 cm<sup>-1</sup>, mean absorption cross-sections of the O<sub>2</sub> Herzberg continuum are used in our computations. The adopted numerical values are given in Table 5.

#### 5. ANALYSIS OF THE PHOTOABSORPTION CROSS-SECTIONS

In our general analysis (Nicolet *et al.*, 1987), the line positions and rotational assignments are reproduced for intervals of 250 cm<sup>-1</sup> and the theoretical and experimental absorption cross-sections are presented graphically (1 cm<sup>-1</sup> per mm) at 300 K throughout the 49,000–57,000 cm<sup>-1</sup> wavenumber region corresponding to all bands with  $v' = 0-19$  and  $v'' = 0$  and 1. This graphical comparison between the calculated and measured absorption cross-sections begins at 49,750 cm<sup>-1</sup>, 1-0 and 3-1 bands, and ends at 55,800 cm<sup>-1</sup>, 12-0 and 19-1 bands.

In order to show the principal features of the spectrum, three different regions (rotational lines with their identifications in Tables 6, 7 and 8) are illustrated in various figures by a semi-logarithmic plot of the absorption cross-sections, namely between 50,500 and 50,750 cm<sup>-1</sup> (Fig. 1a), 51,750 and 52,000 cm<sup>-1</sup> (Fig. 2a), and 54,000 and 54,250 cm<sup>-1</sup> (Fig. 3a). Such

TABLE 4. ADOPTED MEAN ROTATION LINEWIDTHS FOR THE SCHUMANN-RUNGE BANDS OF O<sub>2</sub>

$v'$	cm <sup>-1</sup>	$v'$	cm <sup>-1</sup>
0	0.1	10	1.0
1	0.9	11	1.4
2	0.6	12	0.8
3	1.8	13	0.5
4	3.6	14	0.5
5	2.0	15	0.5
6	1.8	16	0.5
7	1.9	17	0.5
8	2.1	18	0.3
9	1.2	19	0.3

TABLE 5. MEAN ABSORPTION CROSS-SECTIONS OF THE O<sub>2</sub> HERZBERG CONTINUUM DEDUCED FROM FORMULA (1)

Interval (cm <sup>-1</sup> )	Cross-sections (cm <sup>2</sup> )	Interval (cm <sup>-1</sup> )	Cross-section (cm <sup>2</sup> )
49,000–49,500	$7.2 \times 10^{-24}$	52,000–52,500	$7.2 \times 10^{-24}$
49,500–50,000	7.4	52,500–53,000	7.0
50,000–50,500	7.5	53,000–53,500	6.7
50,500–51,000	7.5	53,500–54,000	6.4
51,000–51,500	7.5	54,000–54,500	6.0
51,500–52,000	7.4	54,500–55,000	5.6

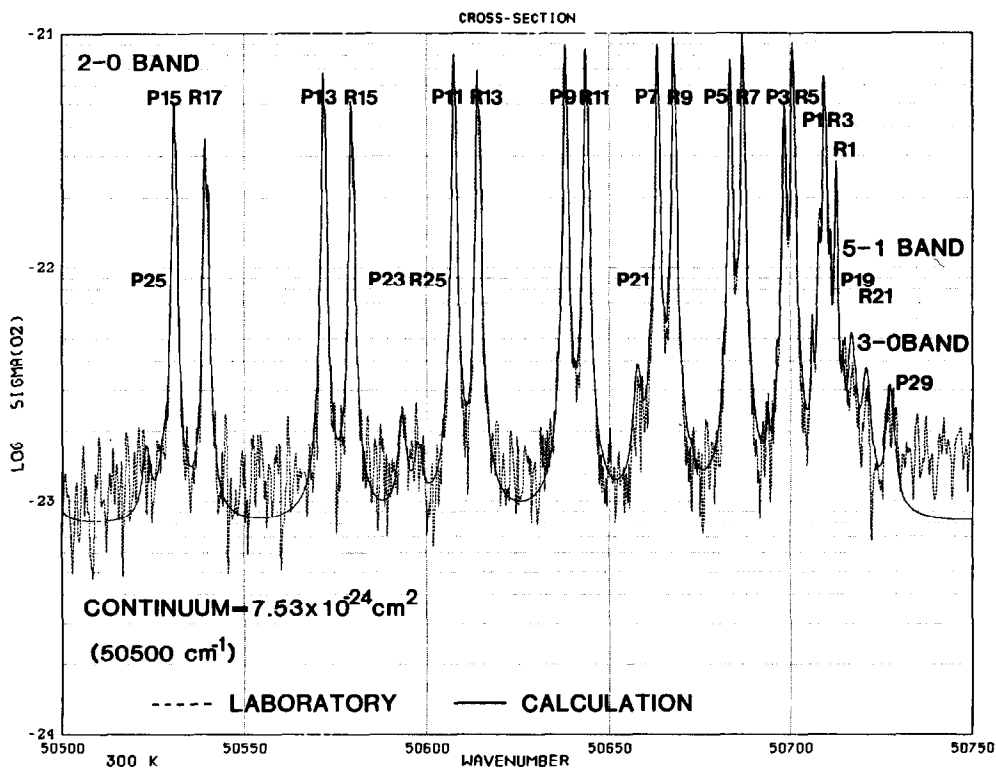


FIG. 1(a). THEORETICAL AND EXPERIMENTAL ABSORPTION CROSS-SECTIONS OF THE 2-0 SCHUMANN-RUNGE BAND OF O<sub>2</sub> BETWEEN 50,500 AND 50,750  $\text{cm}^{-1}$  AT 300 K. Oscillator strength and linewidth are  $1.9 \times 10^{-8}$  and  $0.6 \text{ cm}^{-1}$ , respectively. Strong effect of the Herzberg continuum.

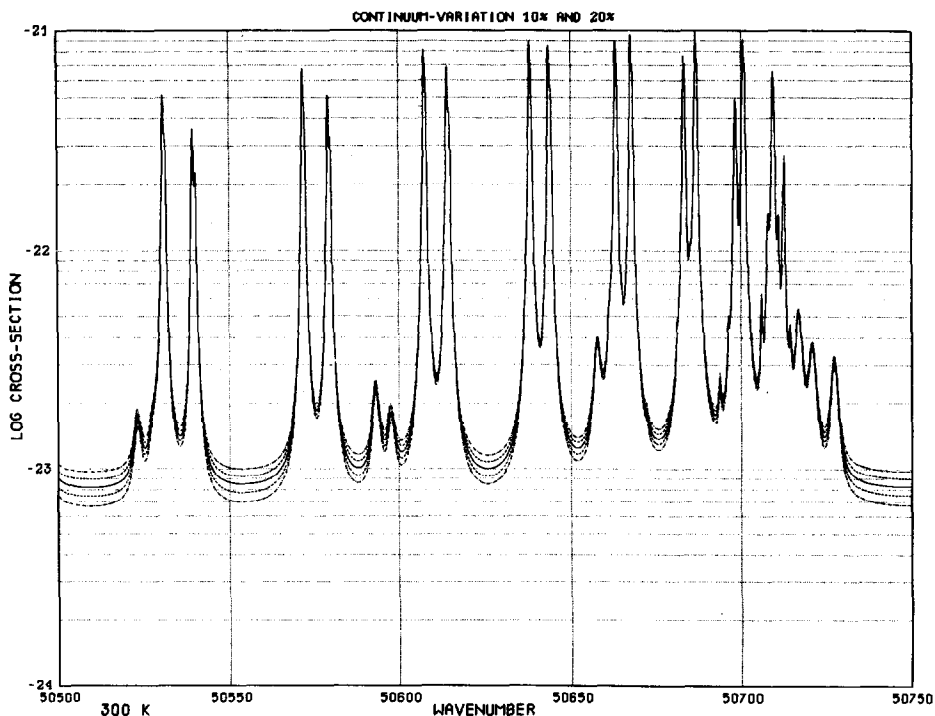


FIG. 1(b). ABSORPTION STRUCTURE OF THE 2-0 BAND WITH VARIATIONS OF  $\pm 10$  AND  $\pm 20\%$  IN THE CROSS-SECTION OF THE UNDERLYING CONTINUUM AT 300 K.

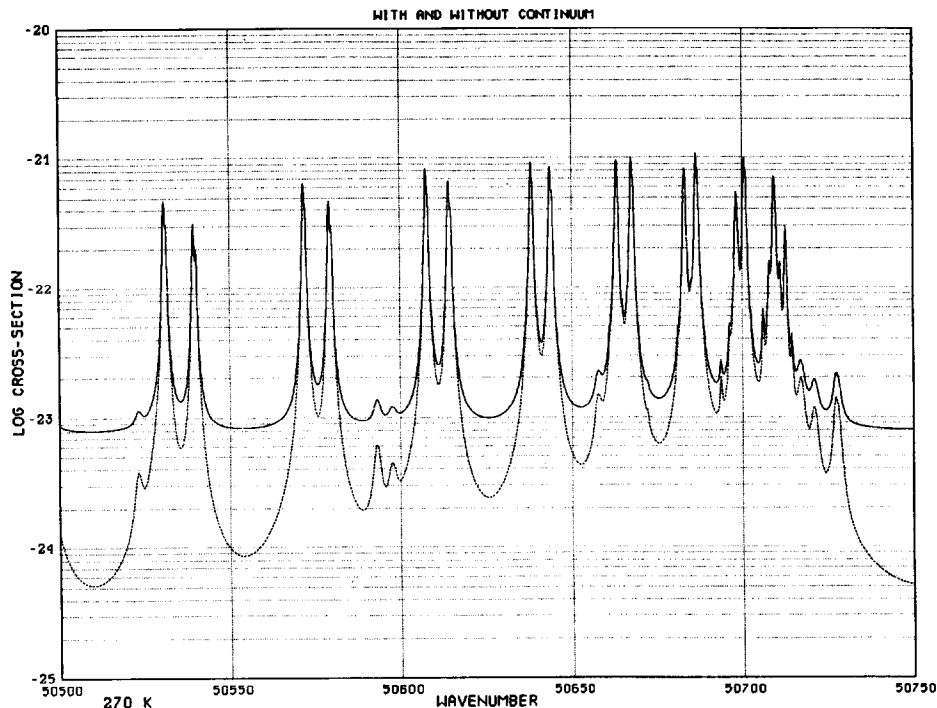


FIG. 1(c). ABSORPTION STRUCTURE WITH AND WITHOUT CONTINUUM BETWEEN 50,500 AND 50,750  $\text{cm}^{-1}$  AT 270 K.  
Differences of a factor of 10 between lines at 50,500  $\text{cm}^{-1}$ .

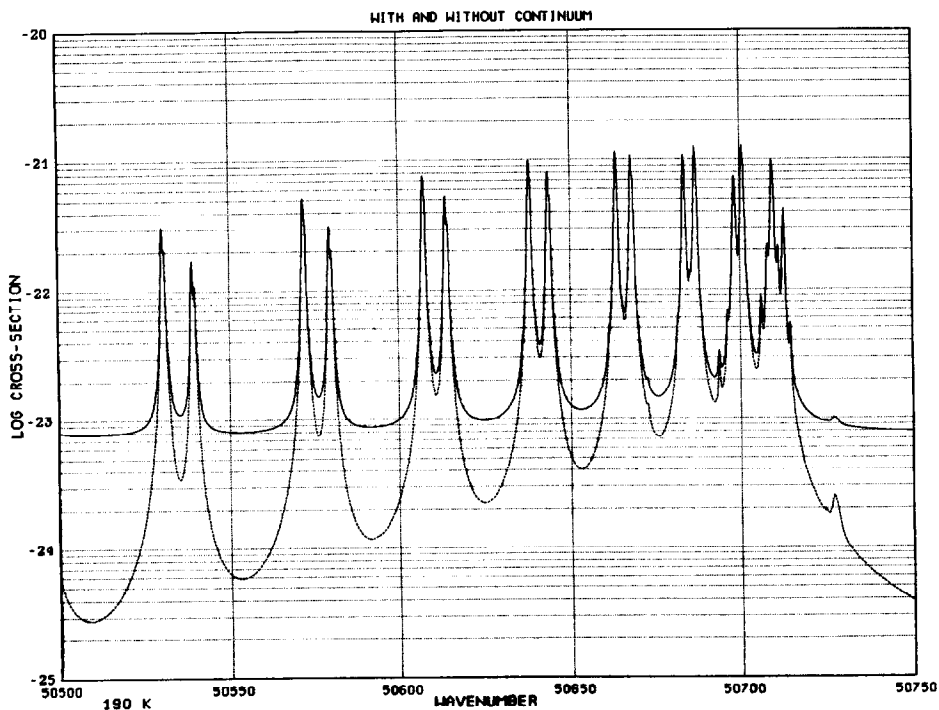


FIG. 1(d). ABSORPTION STRUCTURE WITH AND WITHOUT CONTINUUM BETWEEN 50,500 AND 50,750  $\text{cm}^{-1}$  AT 190 K.  
Increase of differences at high rotation levels; cross-sections reaching  $3 \times 10^{-25} \text{ cm}^2$  near 50,500  $\text{cm}^{-1}$ .

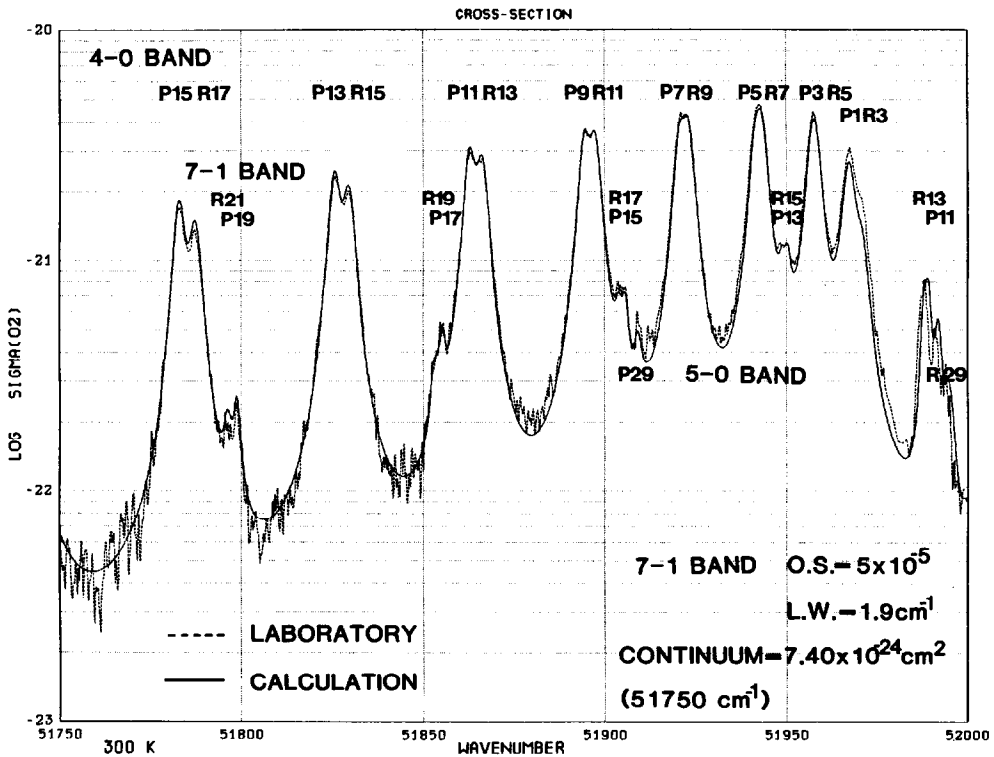


FIG. 2(a). THEORETICAL AND EXPERIMENTAL ABSORPTION CROSS-SECTIONS OF THE 4-0 SCHUMANN-RUNGE BAND OF O<sub>2</sub> BETWEEN 51,750 AND 52,000 cm<sup>-1</sup> AT 300 K. Oscillator strength and linewidth are  $2.7 \times 10^{-7}$  and  $3.6 \text{ cm}^{-1}$ , respectively. Linewidths of 2-0 to be compared.

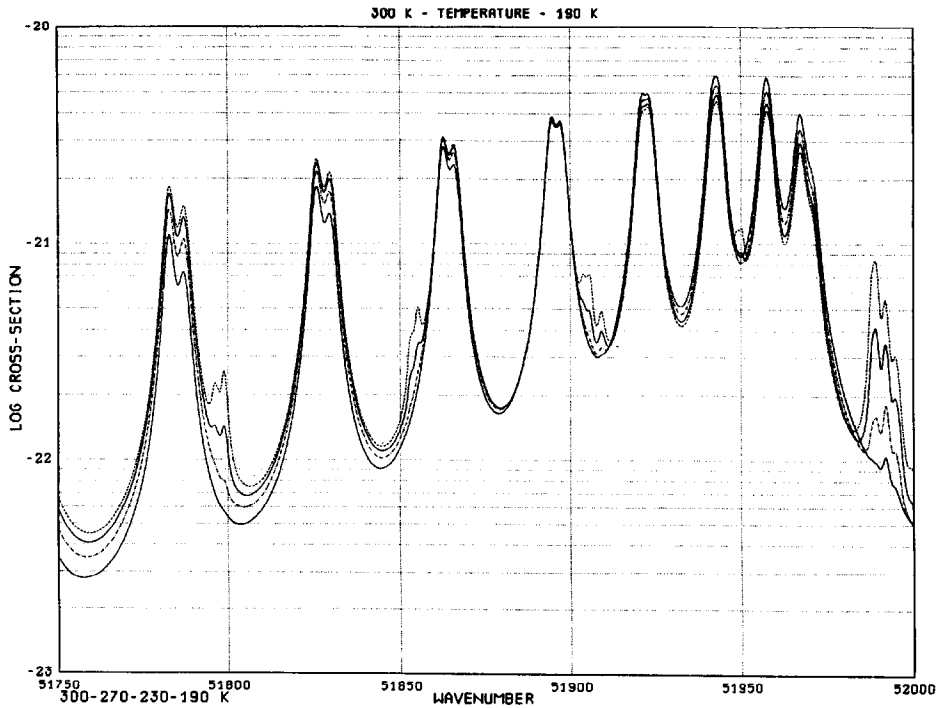


FIG. 2(b). TEMPERATURE EFFECT ON THE ROTATIONAL STRUCTURE BETWEEN 51,750 AND 52,000 cm<sup>-1</sup>. Effects of a temperature decrease from 300 to 270, 230 and 190 K on the 4-0 and 7-1 bands.

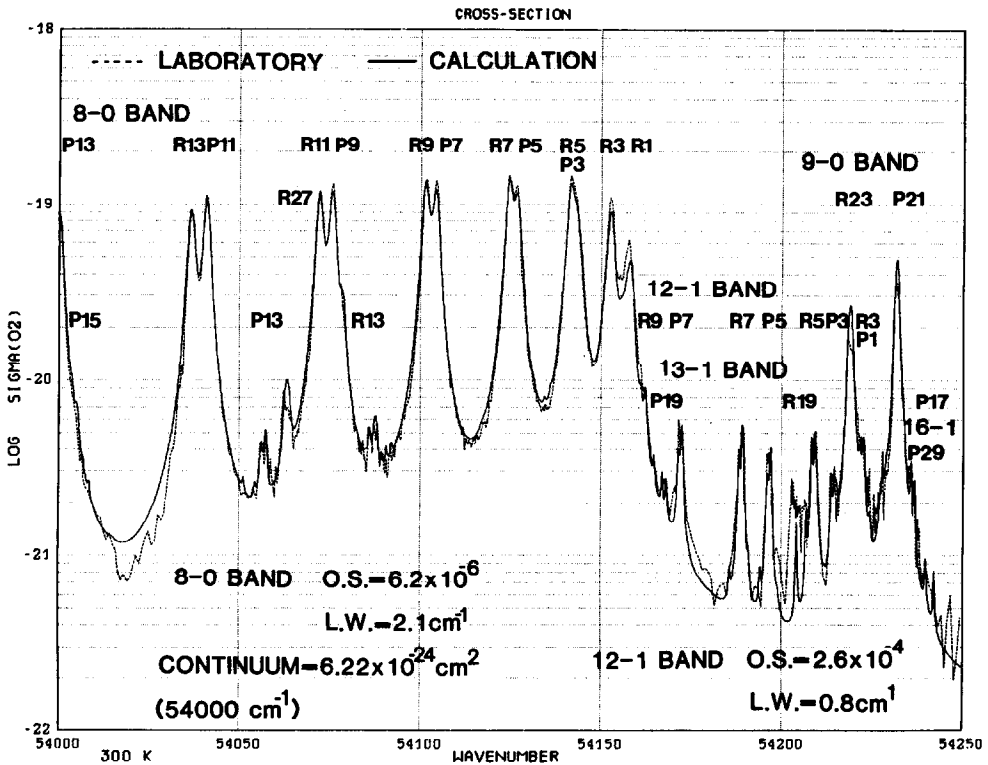


FIG. 3(a). THEORETICAL AND EXPERIMENTAL ABSORPTION CROSS-SECTIONS OF THE 8-0 SCHUMANN-RUNGE BAND OF  $O_2$  BETWEEN  $54,000$  AND  $54,250 \text{ cm}^{-1}$  AT  $300 \text{ K}$ .  
No effect of the underlying continuum.

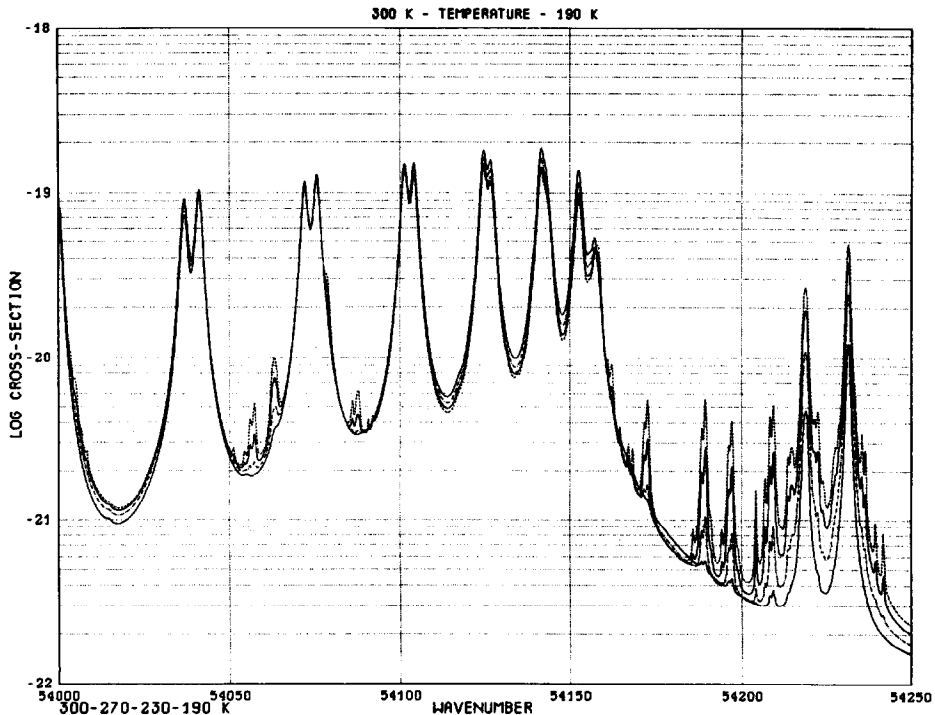


FIG. 3(b). TEMPERATURE EFFECT ON THE ROTATIONAL STRUCTURE BETWEEN  $54,000$  AND  $54,250 \text{ cm}^{-1}$ .  
Effects of a temperature decrease from  $300$  to  $270$ ,  $230$  and  $190 \text{ K}$  particularly on the lines of the 12-1 and 13-1 bands.



figures (Figs 1a, 2a and 3a) make it possible to perform a detailed comparison at 300 K between the calculated and measured cross-sections. The calculations also make it possible to determine the respective role of the lines and of the continuum in the O<sub>2</sub> absorption cross-section (Fig. 1b) where variations of  $\pm 10$  and  $\pm 20\%$  in the underlying continuum are depicted. Other figures have been published for temperature between 270 and 190 K (examples, Figs 1c and 1d) in order to define for each spectral interval the exact role

of the underlying continuum at varying temperatures adopted to atmospheric conditions. Finally, Figs 2b and 2c illustrate the variations in the structure of the absorption spectrum from the laboratory temperature 300 K to atmospheric temperatures 270, 230 and 190 K. It is easy to follow, with decreasing temperature, the marked variations in the absorption of the rotation lines starting from the vibrational level  $v'' = 1$ .

The spectral interval 50,500–50,750 cm<sup>-1</sup> (Table 6

TABLE 6. IDENTIFICATION OF O<sub>2</sub> SHUMANN–RUNGE ROTATIONAL LINES 50500–50750 cm<sup>-1</sup>

$\nu$	$\lambda$	band	$\nu$	$\lambda$	band
<b>50500</b>					
50522.9	1979.30	5-1 P25	50663.3	1973.82	2-0 P 7
50523.0	1979.29	5-1 P25	50663.6	1973.80	2-0 P 7
50523.6	1979.27	5-1 P25	50667.7	1973.64	2-0 R 9
50527.4	1979.13	5-1 R27	50667.7	1973.64	2-0 R 9
50527.7	1979.11	5-1 R27	50668.3	1973.62	2-0 R 9
50528.5	1979.08	5-1 R27	50683.3	1973.04	2-0 P 5
50530.7	1978.99	2-0 P15	50683.4	1973.03	2-0 P 5
50530.7	1978.99	2-0 P15	50683.7	1973.02	2-0 P 5
50531.3	1978.97	2-0 P15	50686.8	1972.90	2-0 R 7
50539.2	1978.66	2-0 R17	50686.8	1972.90	2-0 R 7
50539.3	1978.66	2-0 R17	50687.3	1972.88	2-0 R 7
50540.1	1978.63	2-0 R17	50698.1	1972.46	2-0 P 3
<b>50550</b>					
50571.7	1977.39	2-0 P13	50698.3	1972.45	2-0 P 3
50571.7	1977.39	2-0 P13	50698.6	1972.44	2-0 P 3
<b>50700</b>					
50572.2	1977.37	2-0 P13	50700.6	1972.37	2-0 R 5
50579.2	1977.10	2-0 R15	50700.6	1972.36	2-0 R 5
50579.3	1977.09	2-0 R15	50701.1	1972.35	2-0 R 5
50580.0	1977.07	2-0 R15	50707.9	1972.08	2-0 P 1
50593.0	1976.56	5-1 P23	50709.1	1972.03	2-0 R 3
50593.1	1976.55	5-1 P23	50709.3	1972.03	2-0 R 3
50593.6	1976.53	5-1 P23	50709.7	1972.01	2-0 R 3
50597.2	1976.39	5-1 R25	50710.9	1971.96	2-0 Q 1
50597.5	1976.38	5-1 R25	50712.5	1971.90	2-0 R 1
50598.2	1976.35	5-1 R25	50712.6	1971.90	2-0 R 1
<b>50600</b>					
50607.4	1976.00	2-0 P11	50716.7	1971.74	5-1 P19
50607.4	1975.99	2-0 P11	50716.7	1971.74	5-1 P19
50607.9	1975.98	2-0 P11	50717.2	1971.72	5-1 P19
50613.9	1975.74	2-0 R13	50720.4	1971.59	5-1 R21
50614.0	1975.74	2-0 R13	50720.6	1971.59	5-1 R21
50614.6	1975.71	2-0 R13	50721.2	1971.56	5-1 R21
50637.9	1974.81	2-0 P 9	50726.9	1971.34	3-0 P29
50638.0	1974.80	2-0 P 9	50727.1	1971.33	3-0 P29
50638.4	1974.79	2-0 P 9	50727.9	1971.30	3-0 P29
50643.4	1974.59	2-0 R11			
50643.5	1974.59	2-0 R11			
50644.1	1974.57	2-0 R11			
<b>50650</b>					
50657.6	1974.04	5-1 P21			
50657.6	1974.04	5-1 P21			
50658.1	1974.02	5-1 P21			
50661.6	1973.88	5-1 R23			
50661.8	1973.87	5-1 R23			
50662.5	1973.85	5-1 R23			
50663.2	1973.82	2-0 P 7			

and Figs 1a, b, c and d) corresponds mainly to the 2–0 band with an effect of the 5–1 band at 300 K. The experimental structure for absorption less than  $2 \times 10^{-23} \text{ cm}^2$  is due to laboratory noise. The effect of the underlying Herzberg continuum is important since it can be detected easily by the differences of  $\pm 10$  and  $\pm 20\%$  illustrated in Fig. 1b, particularly by the absolute values of the absorption cross-section with and without continuum at 270 and 190 K as depicted in Figs 1c and 1d.

The spectral interval 51,750–52,000  $\text{cm}^{-1}$  is characterized by linewidths ( $\Delta\nu = 3.6 \text{ cm}^{-1}$ ) of the rotational lines of the 4–0 band (Table 7). These lines play a very important role in the overall pattern of absorption (Fig. 2a), since the effect of the Herzberg continuum is negligible and produces practically no variation when the absorption cross-section is varied by  $\pm 10$  or  $\pm 20\%$ . The variation of the absorption cross-section with temperature ( $T = 300, 270, 230$ –190 K) illustrates the decreasing role of the 7–1 band

TABLE 7. IDENTIFICATION OF O<sub>2</sub> SCHUMANN–RUNGE ROTATIONAL LINES 51750–52000  $\text{cm}^{-1}$

$\nu$	$\lambda$	band	$\nu$	$\lambda$	band
51750					
51782.7	1931.15	4-0 P15	51909.1	1926.45	5-0 P29
51782.9	1931.14	4-0 P15	51909.7	1926.42	5-0 P29
51783.4	1931.12	4-0 P15	51911.4	1926.36	8-1 P29
51787.1	1930.98	4-0 R17	51911.9	1926.34	8-1 P29
51787.4	1930.97	4-0 R17	51912.5	1926.32	8-1 P29
51788.0	1930.95	4-0 R17	51920.5	1926.02	4-0 P 7
51796.0	1930.65	7-1 R21	51920.6	1926.02	4-0 P 7
51796.3	1930.64	7-1 R21	51920.9	1926.01	4-0 P 7
51797.0	1930.61	7-1 R21	51922.9	1925.93	4-0 R 9
51798.7	1930.55	7-1 P19	51923.0	1925.93	4-0 R 9
51798.8	1930.55	7-1 P19	51923.5	1925.91	4-0 R 9
51799.3	1930.53	7-1 P19	51941.3	1925.25	4-0 P 5
51800			51941.3	1925.25	4-0 P 5
51825.4	1929.56	4-0 P13	51941.7	1925.24	4-0 P 5
51825.5	1929.55	4-0 P13	51943.1	1925.18	4-0 R 7
51826.0	1929.54	4-0 P13	51943.2	1925.18	4-0 R 7
51829.3	1929.41	4-0 R15	51943.6	1925.16	4-0 R 7
51829.5	1929.40	4-0 R15	51948.6	1924.98	7-1 R15
51830.1	1929.38	4-0 R15	51948.8	1924.97	7-1 R15
51850			51949.3	1924.96	7-1 R15
51852.7	1928.54	7-1 R19	51950		
51853.0	1928.53	7-1 R19	51950.2	1924.92	7-1 P13
51853.6	1928.51	7-1 R19	51950.3	1924.92	7-1 P13
51855.0	1928.46	7-1 P17	51950.6	1924.90	7-1 P13
51855.1	1928.45	7-1 P17	51956.6	1924.68	4-0 P 3
51855.5	1928.43	7-1 P17	51956.6	1924.68	4-0 P 3
51862.6	1928.17	4-0 P11	51957.1	1924.67	4-0 P 3
51862.6	1928.17	4-0 P11	51957.9	1924.64	4-0 R 5
51863.1	1928.15	4-0 P11	51957.9	1924.63	4-0 R 5
51865.9	1928.05	4-0 R13	51958.4	1924.62	4-0 R 5
51866.1	1928.04	4-0 R13	51966.4	1924.32	4-0 P 1
51866.7	1928.02	4-0 R13	51967.2	1924.29	4-0 R 3
51894.3	1926.99	4-0 P 9	51967.2	1924.29	4-0 R 3
51894.3	1926.99	4-0 P 9	51967.6	1924.27	4-0 R 3
51894.7	1926.98	4-0 P 9	51969.4	1924.21	4-0 Q 1
51897.1	1926.89	4-0 R11	51971.0	1924.15	4-0 R 1
51897.3	1926.88	4-0 R11	51971.0	1924.15	4-0 R 1
51897.8	1926.86	4-0 R11	51987.8	1923.53	7-1 R13
51900			51987.9	1923.52	7-1 R13
51903.6	1926.65	7-1 R17	51988.4	1923.51	7-1 R13
51903.8	1926.64	7-1 R17	51989.1	1923.48	7-1 P11
51904.3	1926.62	7-1 R17	51989.1	1923.48	7-1 P11
51905.5	1926.58	7-1 P15	51989.5	1923.47	7-1 P11
51905.6	1926.57	7-1 P15	51989.7	1923.46	8-1 R29
51906.0	1926.56	7-1 P15	51990.4	1923.43	8-1 R29
51908.9	1926.45	5-0 P29	51991.2	1923.40	8-1 R29

(Fig. 2b) and the change in the structure of the 4–0 band at high rotational levels, P15–R17.

In the 54,000–54,250  $\text{cm}^{-1}$  interval, the principal contribution to the total absorption cross-section to the P1–P13 lines of the 8–0 band with an additional effect of the 12–1 and 13–1 bands (Fig. 3a). There is no contribution of the continuum ( $6 \times 10^{-24} \text{ cm}^2$ ) since the minimum cross-section is not less than  $5 \times 10^{-22} \text{ cm}^2$ . The variation of the structure (Fig. 3b) is associated only with the rotational and vibrational populations related to temperatures 300–190 K, particularly in the 54,150–54,250  $\text{cm}^{-1}$  region corresponding to the lines of the (12–1), (13–1) and (14–1) bands.

It seems, therefore, that there is a remarkable agreement between the experimental and theoretical cross-sections. Yoshino *et al.* (1983) estimate that the error in the spectral range 6–0 to 12–0 bands may vary from about 5% in regions of the principal absorption peaks to about 10% in window regions and that errors in the range of the absolute cross-sections below  $10^{-22} \text{ cm}^2$  could be somewhat greater. In any case, our detailed modeling procedure in which the cross-section

is computed as a function of wavenumber for lines with Voigt profiles and in which predissociation line widths are treated as parameters produces excellent agreement with the best experimental data independent of the instrumental width. It is also justified by a comparison of the theoretical and experimental cross-sections at 79 K.

#### 6. THE SCHUMANN–RUNGE BANDS AT 79 K

The recent experimental determination by Yoshino *et al.* (1987) of the cross-sections at 79 K with an instrumental bandwidth of  $0.4 \text{ cm}^{-1}$  has been compared with a theoretical calculation based on the spectroscopic parameters adopted at 300 K. We present our comparison in graphical format with a semi-logarithmic plot for the 2–0 bands through 12–0 with a complete assignment of all rotation lines (Figs 4–14). According to Yoshino *et al.* (1987), their experimental values of the absolute absorption cross-sections would be of the order of 4% in regions of the principal absorption peaks while the errors in the range below  $5 \times 10^{-22} \text{ cm}^{-1}$  should be greater (limited column den-

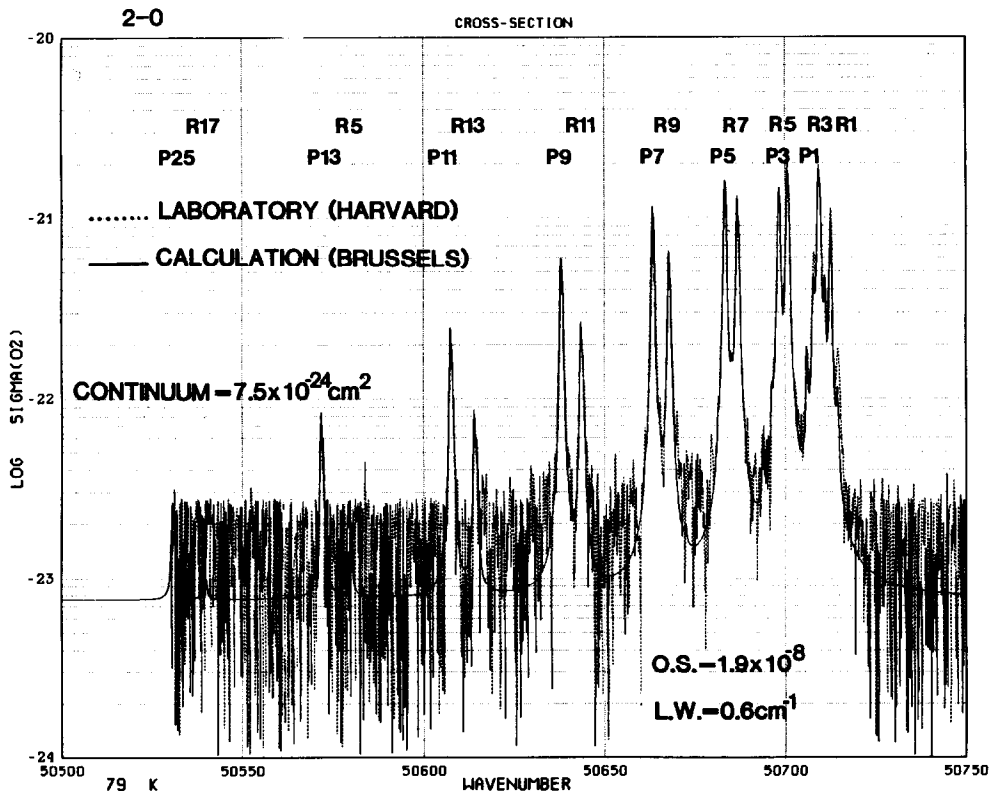


FIG. 4. ABSORPTION CROSS-SECTIONS OF THE 2–0 BAND AT 79 K.

Experimental cross-sections less than  $5 \times 10^{-23} \text{ cm}^2$  in the laboratory noise. Agreement between theoretical and experimental peaks.

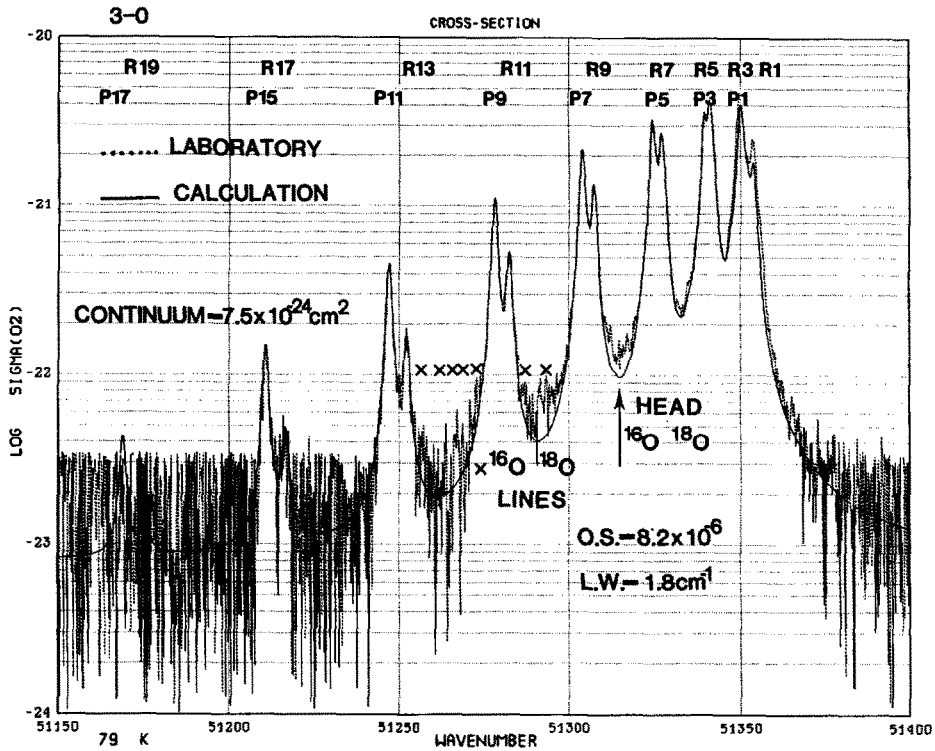


FIG. 5. ABSORPTION CROSS-SECTIONS OF THE 3-0 BAND AT 79 K.  
Rotation lines of  $^{16}\text{O}^{18}\text{O}$  isotope with spikes for cross-sections not less than  $5 \times 10^{-23} \text{ cm}^2$ .

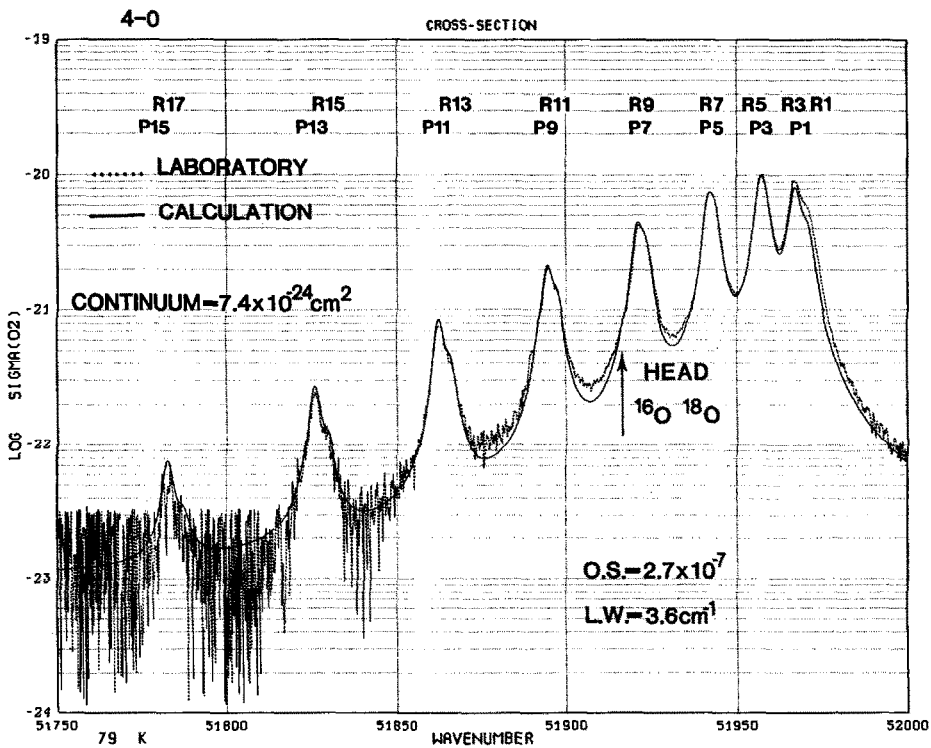


FIG. 6. ABSORPTION CROSS-SECTIONS OF THE 4-0 BAND AT 79 K.  
Linewidth determined at 300 K in agreement with structure at 79 K.

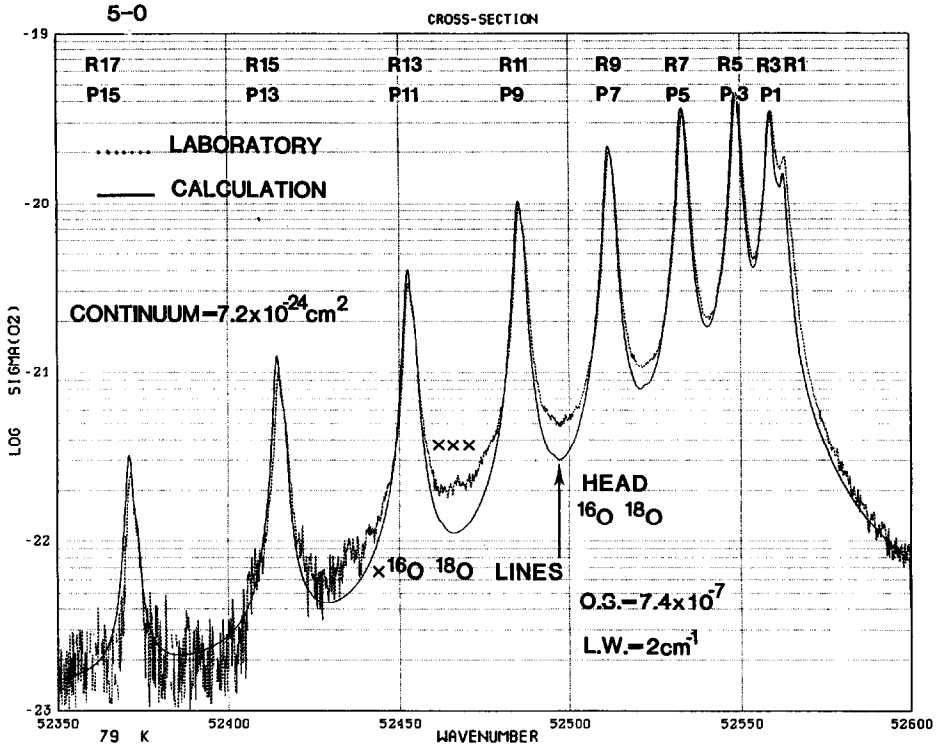


FIG. 7. ABSORPTION CROSS-SECTIONS OF THE 5-0 BAND AT 79 K. Underlying continuum ( $0.7 \times 10^{-23} \text{ cm}^2$ ) without any effect.

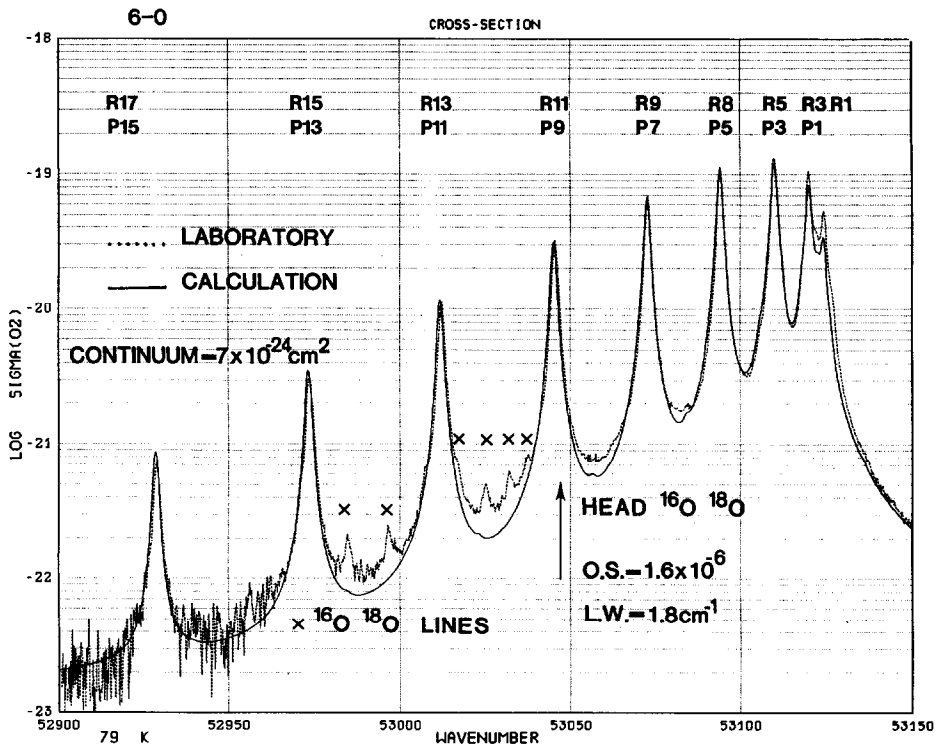


FIG. 8. ABSORPTION CROSS-SECTIONS OF THE 6-0 BAND AT 79 K. Spikes corresponding to <sup>16</sup>O<sup>18</sup>O lines clearly apparent between <sup>16</sup>O<sub>2</sub> lines below the <sup>16</sup>O<sup>18</sup>O head.

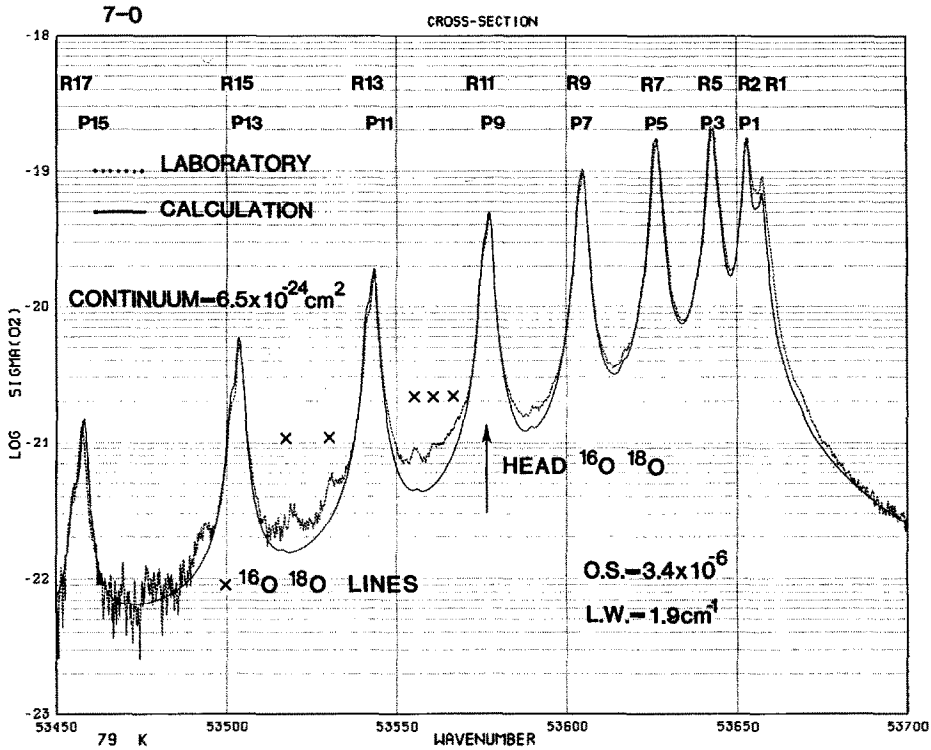


FIG. 9. ABSORPTION CROSS-SECTIONS OF THE 7-0 BAND AT 79 K. Laboratory noise still noticeable near  $10^{-22} \text{ cm}^2$ .

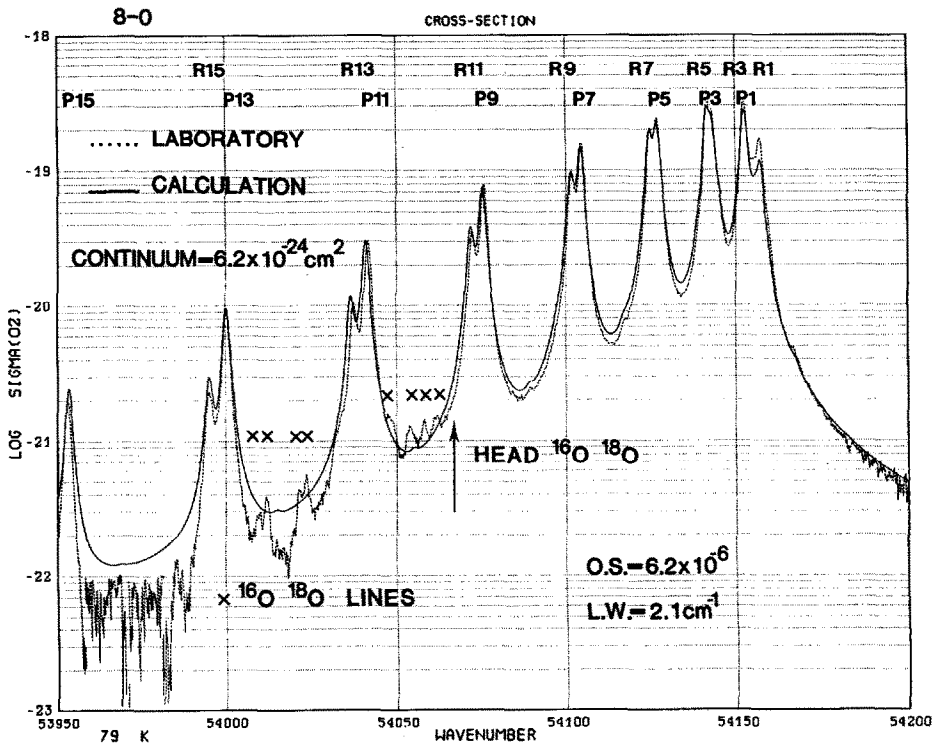


FIG. 10. ABSORPTION CROSS-SECTIONS OF THE 8-0 BAND AT 79 K. Apparent anomaly between P13 and P15 lines as a result of the laboratory limited column density.

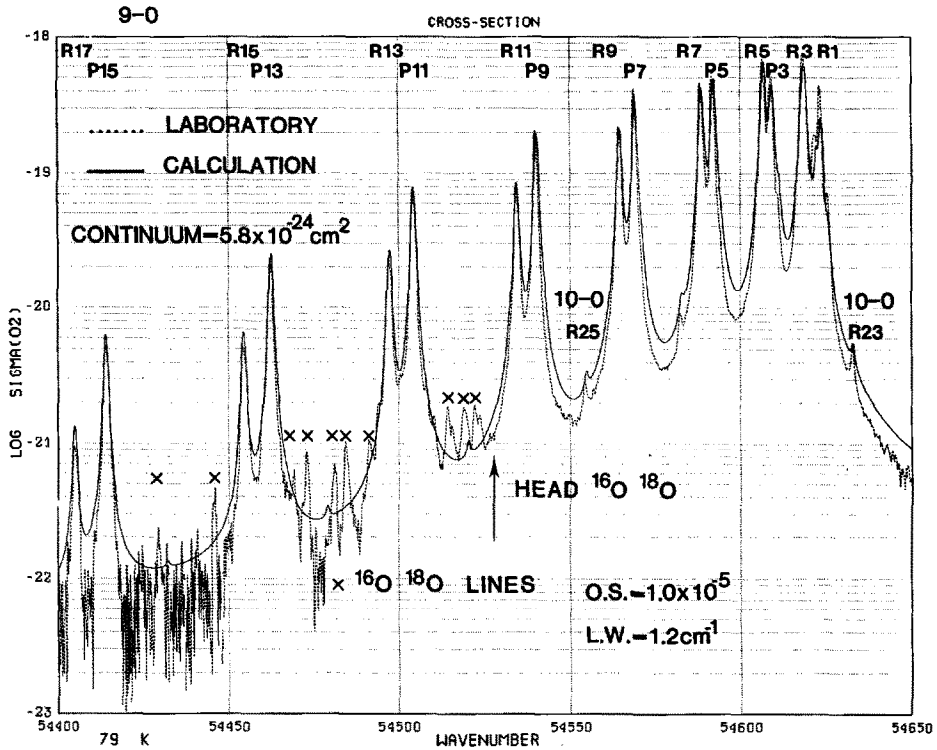


FIG. 11. ABSORPTION CROSS-SECTIONS OF THE 9-0 BAND AT 79 K. Superposition between P13 and R13 lines of  $^{16}\text{O}^{18}\text{O}$  spikes and laboratory noise,  $> 5 \times 10^{-22} \text{ cm}^2$  and  $< 10^{-22} \text{ cm}^2$ , respectively.

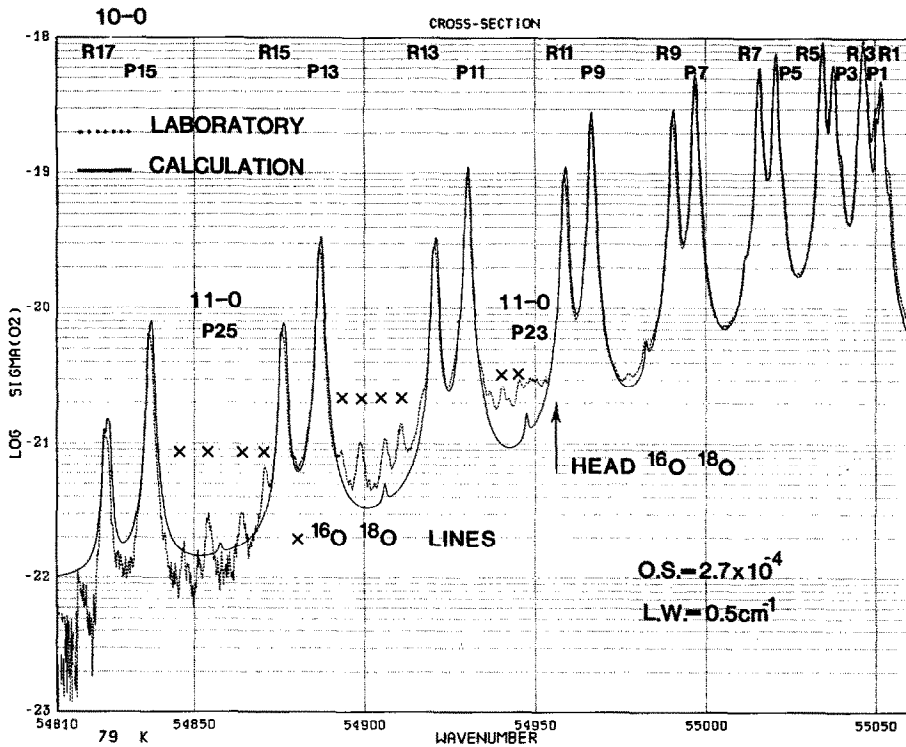


FIG. 12. ABSORPTION CROSS-SECTIONS OF THE 10-0 BAND AT 79 K. All aspects described in Figs 4-10 present in a comparison of theoretical and experimental structures.

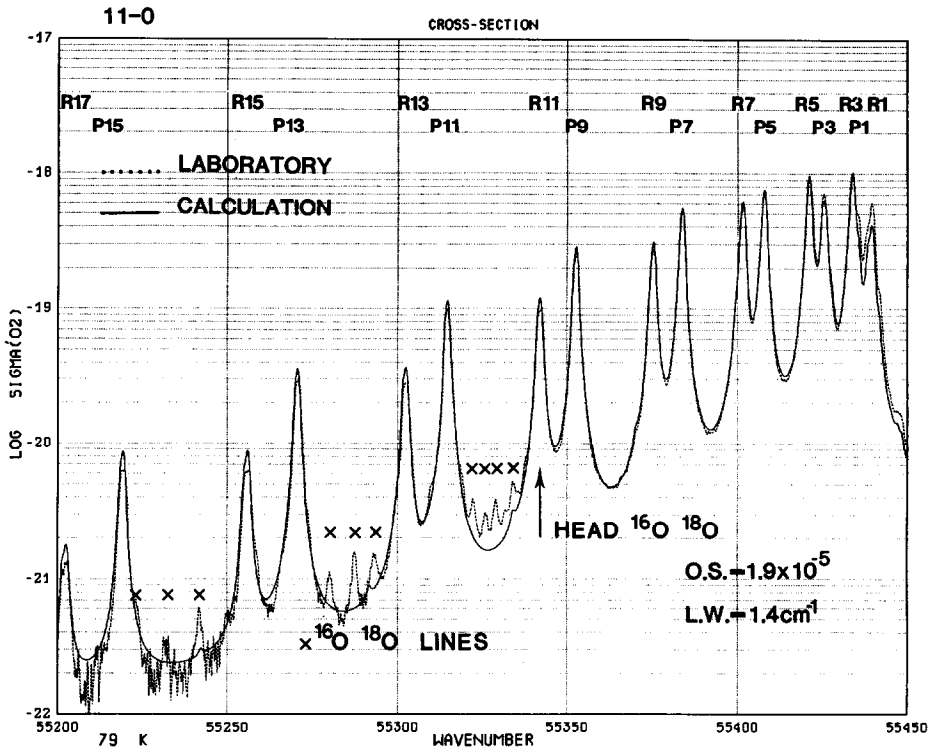


FIG. 13. ABSORPTION CROSS-SECTIONS OF THE 11-0 BAND AT 79 K.  
Remarkable differences in structure above and below <sup>16</sup>O<sup>18</sup>O head.

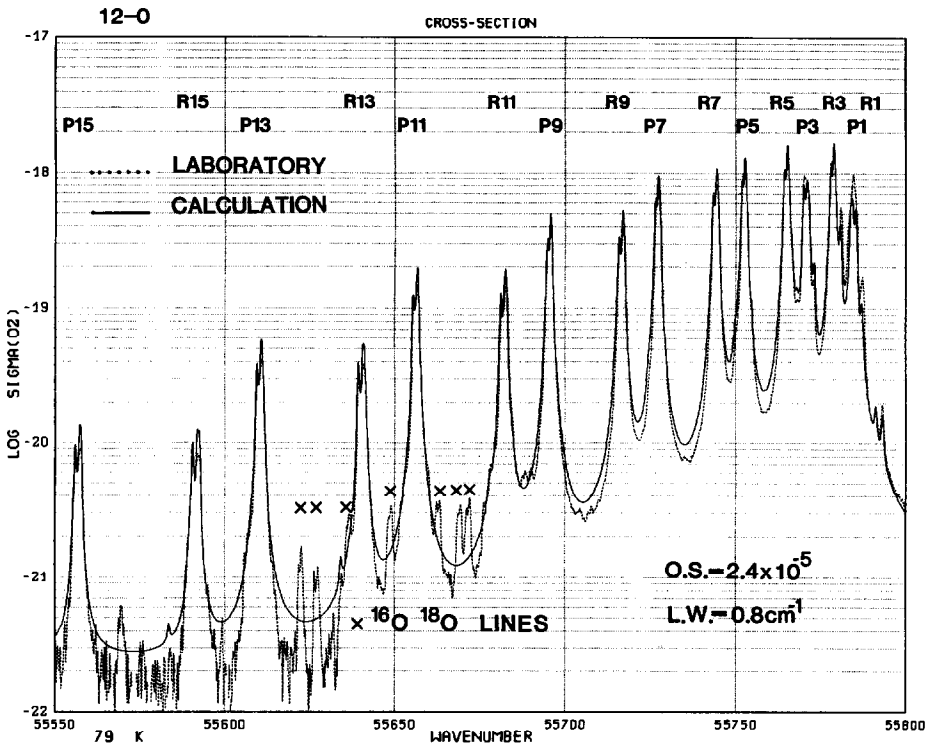


FIG. 14. ABSORPTION CROSS-SECTIONS OF THE 12-0 BAND AT 79 K.  
Last band with experimental cross-sections.



TABLE 8. IDENTIFICATION OF O<sub>2</sub> SCHUMANN-RUNGE ROTATIONAL LINES 54000–54250 cm<sup>-1</sup>

$\nu$	$\lambda$	band	$\nu$	$\lambda$	band	$\nu$	$\lambda$	band
54000								
54000.0	1851.85	8-0 P13	54092.9	1848.67	15-1 P29	54153.1	1846.62	8-0 P 1
54000.2	1851.85	8-0 P13	54094.3	1848.62	14-1 R27	54153.1	1846.62	15-1 R29
54000.5	1851.84	8-0 P13	54100			54155.8	1846.52	8-0 Q 1
54003.7	1851.73	12-1 P15	54100.8	1848.40	15-1 P29	54157.2	1846.48	8-0 R 1
54004.9	1851.68	12-1 P15	54101.1	1848.39	8-0 R 9	54157.4	1846.47	8-0 R 1
54005.4	1851.67	12-1 P15	54101.3	1848.39	8-0 R 9	54158.0	1846.45	9-0 P23
54006.9	1851.62	13-1 P23	54101.4	1848.38	12-1 P11	54158.4	1846.44	9-0 P23
54008.5	1851.56	13-1 P23	54101.6	1848.38	8-0 R 9	54158.7	1846.43	9-0 P23
54035.9	1850.62	14-1 P27	54102.5	1848.34	12-1 P11	54161.1	1846.35	12-1 R 9
54036.4	1850.61	8-0 R13	54102.7	1848.34	12-1 P11	54162.1	1846.31	12-1 R 9
54036.6	1850.60	8-0 R13	54104.0	1848.29	8-0 P 7	54162.4	1846.30	12-1 R 9
54037.0	1850.59	8-0 R13	54104.1	1848.29	8-0 P 7	54164.6	1846.22	13-1 P19
54038.0	1850.55	12-1 R15	54104.4	1848.28	8-0 P 7	54167.0	1846.14	13-1 P19
54039.4	1850.50	12-1 R15	54124.3	1847.60	8-0 R 7	54168.1	1846.10	13-1 P19
54040.0	1850.48	12-1 R15	54124.4	1847.59	8-0 R 7	54171.5	1845.99	12-1 P 7
54040.8	1850.45	8-0 P11	54124.7	1847.58	8-0 R 7	54172.4	1845.96	12-1 P 7
54040.9	1850.45	14-1 P27	54126.5	1847.52	8-0 P 5	54172.5	1845.96	12-1 P 7
54041.2	1850.44	8-0 P11	54126.6	1847.52	8-0 P 5	54185.8	1845.50	14-1 R25
54044.0	1850.34	14-1 P27	54126.9	1847.51	8-0 P 5	54188.2	1845.42	12-1 R 7
54050			54127.0	1847.51	12-1 R11	54189.2	1845.39	12-1 R 7
54051.2	1850.10	13-1 R23	54128.2	1847.47	12-1 R11	54189.4	1845.38	12-1 R 7
54054.4	1849.99	13-1 R23	54128.6	1847.45	12-1 R11	54190.9	1845.33	14-1 R25
54056.0	1849.93	12-1 P13	54131.5	1847.35	13-1 R21	54194.1	1845.22	14-1 R25
54056.5	1849.92	13-1 R23	54134.4	1847.26	13-1 R21	54196.1	1845.15	12-1 P 5
54057.2	1849.89	12-1 P13	54136.1	1847.20	13-1 R21	54197.0	1845.12	12-1 P 5
54057.5	1849.88	12-1 P13	54138.6	1847.11	15-1 R29	54197.1	1845.12	12-1 P 5
54062.6	1849.71	9-0 R27	54139.8	1847.07	14-1 P25	54200		
54063.2	1849.69	9-0 R27	54139.9	1847.07	12-1 P 9	54204.2	1844.88	13-1 R19
54063.7	1849.67	9-0 R27	54140.9	1847.03	12-1 P 9	54206.9	1844.79	13-1 R19
54071.8	1849.39	8-0 R11	54141.0	1847.03	12-1 P 9	54208.4	1844.73	13-1 R19
54072.0	1849.39	8-0 R11	54141.4	1847.02	8-0 R 5	54208.4	1844.73	12-1 R 5
54072.3	1849.38	8-0 R11	54141.5	1847.01	8-0 R 5	54209.3	1844.70	12-1 R 5
54075.5	1849.27	8-0 P 9	54141.8	1847.00	8-0 R 5	54209.5	1844.70	12-1 R 5
54075.6	1849.26	8-0 P 9	54142.9	1846.96	8-0 P 3	54210.7	1844.65	15-1 P27
54075.9	1849.25	8-0 P 9	54143.0	1846.96	8-0 P 3	54213.8	1844.55	12-1 P 3
54078.2	1849.17	9-0 P25	54143.5	1846.94	8-0 P 3	54214.7	1844.52	12-1 P 3
54078.7	1849.16	9-0 P25	54143.7	1846.94	9-0 R25	54215.2	1844.50	12-1 P 3
54079.0	1849.15	9-0 P25	54144.3	1846.92	9-0 R25	54217.5	1844.42	16-1 P29
54084.9	1848.95	14-1 R27	54144.4	1846.91	14-1 P25	54217.9	1844.41	15-1 P27
54086.0	1848.91	12-1 R13	54144.7	1846.90	9-0 R25	54218.4	1844.39	9-0 R23
54087.3	1848.86	12-1 R13	54147.1	1846.82	14-1 P25	54219.0	1844.37	9-0 R23
54087.8	1848.85	12-1 R13	54147.4	1846.81	15-1 R29	54219.4	1844.36	9-0 R23
54088.0	1848.84	13-1 P21	54150			54221.6	1844.28	12-1 R 3
54090.6	1848.75	14-1 R27	54152.4	1846.64	8-0 R 3	54222.2	1844.26	15-1 P27
54090.6	1848.75	13-1 P21	54152.5	1846.64	8-0 R 3	54222.5	1844.25	12-1 R 3
54092.0	1848.70	13-1 P21	54152.9	1846.62	8-0 R 3	54222.8	1844.24	12-1 R 3

sity). This is the explanation of the strong noise (logarithmic scale) in the figures corresponding to 2–0 and 3–0 where the continuum cross-section is less than  $5 \times 10^{-23}$  cm<sup>2</sup>.

Spikes which are clearly apparent in the experimental data, from the 6–0 to 12–0 bands, between the principal lines shown with their assignments are mostly rotational lines of the isotopic molecules <sup>16</sup>O<sup>18</sup>O. These spectral features are shown in the vari-

ous figures with an indication of the heads of the <sup>16</sup>O<sup>18</sup>O bands. We have verified our assignments thanks to unpublished data (Yoshino-Egmont, personal communication). As an example, the cross-sections of the 8–0 bands of <sup>16</sup>O<sub>2</sub> and <sup>16</sup>O<sup>18</sup>O are compared in Fig. 15. It is clear that the four spikes (see Fig. 10) in the window between the P9 and P11 lines of <sup>16</sup>O<sub>2</sub> near 54,050 cm<sup>-1</sup> correspond to the first lines of the <sup>16</sup>O<sup>18</sup>O molecules and that the two groups

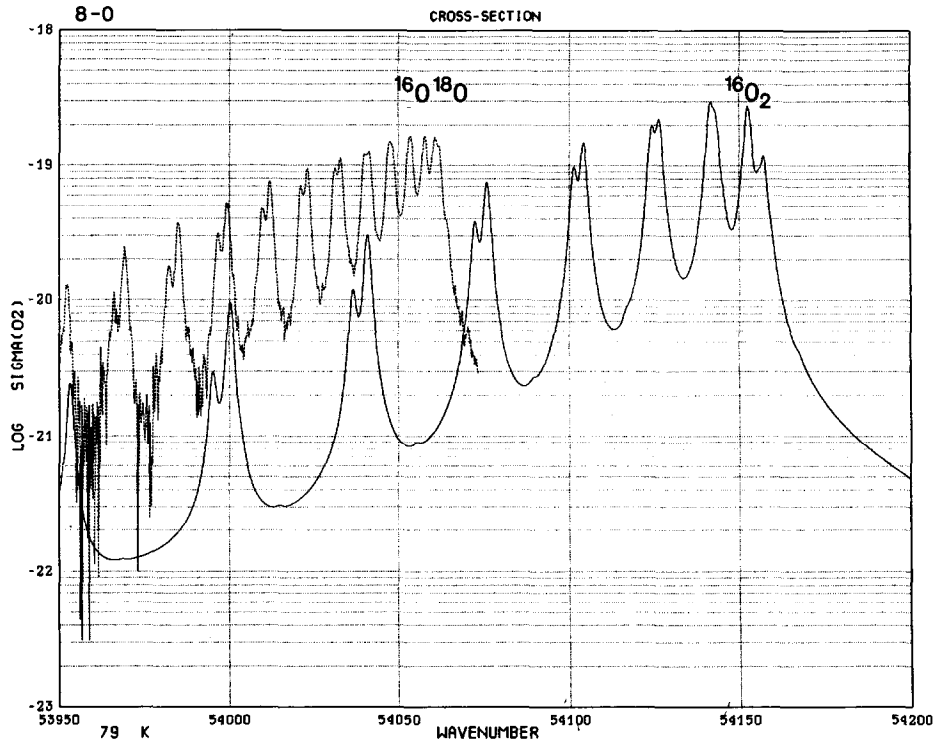


FIG. 15. ABSORPTION CROSS-SECTIONS OF THE  $^{16}\text{O}_2$  AND  $^{16}\text{O}^{18}\text{O}$  BANDS AT 79 K. Comparison between  $^{16}\text{O}^{18}\text{O}$  experimental and  $^{16}\text{O}_2$  theoretical determinations.

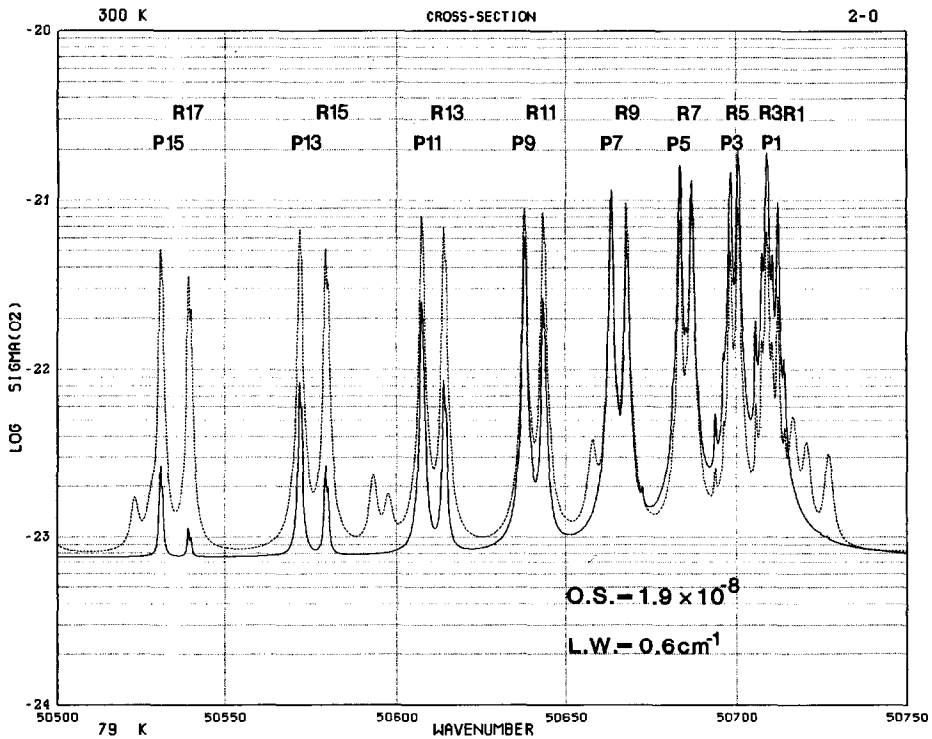


FIG. 16. ROTATIONAL STRUCTURES OF THE 2-0 BAND AT 300 AND 79 K. At high rotational levels, upper curve for 300 K and lower curve for 79 K. At P7-R9 lines, beginning of an inverted position for both curves.

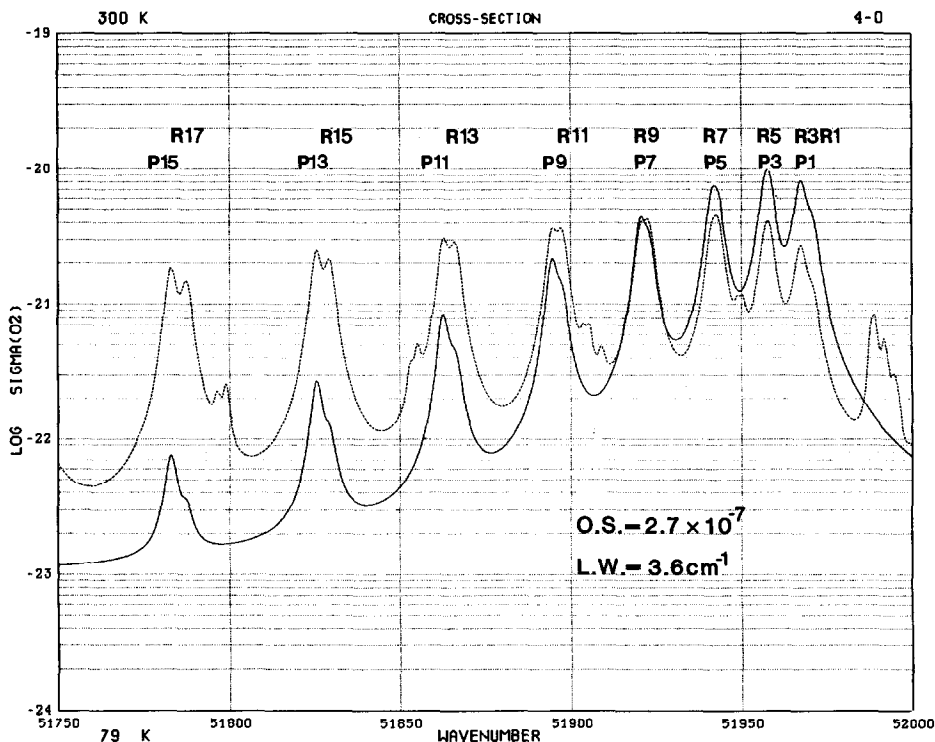


FIG. 17. ROTATIONAL STRUCTURES OF THE 4-0 BAND AT 300 AND 79 K. At high rotational levels, upper curve for 300 K and lower curve for 79 K. At P7-R9 lines, beginning of an inverted position for both curves.

with a double structure between the P11 and P13 lines of  $^{16}\text{O}_2$ , near  $54,025\text{ cm}^{-1}$  belong to the  $^{16}\text{O}^{18}\text{O}$  isotopic molecule.

#### 7. COMPARISON BETWEEN THE ABSORPTION STRUCTURES AT 300 AND 79 K

The theoretical cross-sections of the (2-0) to (12-0) bands at 300 and 79 K have been compared. Two examples are shown in Figs 16 and 17 for the 2-0 and 4-0 bands. Details of the line assignments (Yoshino *et al.*, 1984; Nicolet *et al.*, 1987) show (see Figs 1a and 2a, respectively) that the main apparent differences are due to the temperature contrast, specifically the disappearance of the lines corresponding to  $v'' = 1$  and the decrease of the intensity of the line corresponding to  $v'' = 0$  at relatively high rotational levels (see Tables 6 and 7). This means that the absorption cross-sections at 79 K as shown in Figs 4-14 are practically free from any lines of other bands, and they increase on the lower rotational levels.

#### 8. CONCLUDING REMARK

The high resolution absorption cross-section measurements made by the Harvard-Smithsonian group at 300 and 79 K of various bands of the Schumann-Runge system of  $\text{O}_2$  have allowed the calculation of linewidths of rotational lines for which the band oscillator strengths were obtained. An accurate calculation of the band structures at various atmospheric temperatures may be performed when adequate averaged linewidths are determined for each band.

*Acknowledgements*—This work is based not only on the most recent publications available, but also on unpublished experimental data. Our special thanks go to the members of the Harvard-Smithsonian Group who have kindly provided such data. Support for the preparation of this work has been facilitated by grants from the Commission of the European Communities, Directorate-General for Science, Research and Development, Environment Research Programme, of the Office of Naval Research contract N0014-86-K-0265-P0002 with the Communications and Space Sciences Laboratory of Penn State University, and of the Chemical Manufacturers Association Contract FC 85-563 with the Institut d'Aéronomie Spatiale.

## REFERENCES

- Ackerman, M. and Biaumé, F. (1970) Structure of the Schumann–Runge bands from the (0–0) to the (13–0) band. *J. Molec. Spectros.* **35**, 73.
- Allison, A., Dalgarno, A. and Pasachoff, N. W. (1971) Absorption by vibrationally-excited molecular oxygen in the Schumann–Runge continuum. *Planet. Space Sci.* **19**, 1463.
- Biaumé, F. (1972) Détermination de la valeur absolue de l'absorption dans les bandes du Système de Schumann–Runge de l'oxygène moléculaire. *Aeronomica Acta, Brussels, A*, no. 100, 1–270.
- Brix, P. and Herzberg, G. (1954) Fine structure of the Schumann–Runge bands near the convergence limit and the dissociation energy of oxygen molecule. *Can. J. Phys.* **32**, 110.
- Cheung, A. S.-C., Yoshino, K., Parkinson, W. H. and Freeman, D. E. (1984) Herzberg continuum cross section of oxygen in the wavelength region 193.5–204.0 nm and band oscillator strength of the (0–0) and (1–0) Schumann–Runge bands. *Can. J. Phys.* **62**, 1752.
- Cheung, A. S.-C., Yoshino, K., Parkinson, W. H. and Freeman, D. E. (1986) Molecular spectroscopic constants of  $O_2(^3\Sigma_u^-)$ , the upper state of the Schumann–Runge bands. *J. molec. Spectrosc.* **119**, 1.
- Fang, T. M., Wofsy, S. C. and Dalgarno, A. (1974) Opacity distribution functions and absorption in Schumann–Runge bands of molecular oxygen. *Planet. Space Sci.* **22**, 413.
- Lewis, B. R., Berzins, L. and Carver, J. H. (1986a) Oscillator strengths for the Schumann–Runge bands of  $^{16}O_2$ . *J. Quant. Spectrosc. Rad. Trans.* **36**, 209.
- Lewis, B. R., Berzins, L., Carver, J. H. and Gibson, S. T. (1985a) Decomposition of the photoabsorption continuum underlying the Schumann–Runge bands of  $^{16}O_2$ —I. Role of the  $B^3\Sigma$  state. I—A new dissociation limit. *J. Quant. Spectrosc. Rad. Trans.* **33**, 627.
- Lewis, B. R., Berzins, L., Carver, J. H. and Gibson, S. T. (1986b) Rotational variation of predissociation linewidth in the Schumann–Runge bands of  $^{16}O_2$ . *J. Quant. Spectrosc. Rad. Trans.* **36**, 187.
- Lewis, B. R., Berzins, L., Carver, J. H., Gibson, S. T. and McCoy, D. G. (1985b) Decomposition of the photoabsorption continuum underlying the Schumann–Runge bands of  $^{16}O_2$ —II. Role of the  $1^3\Pi$  state and collision induced absorption. *J. Quant. Spectrosc. Rad. Trans.* **34**, 405.
- Nicolet, M., Cieslik, S. and Kennes, R. (1987) Rotational structure and absorption cross sections from 300 K to 190 K of the Schumann–Runge bands of  $O_2$ . *Aeronomica Acta, Brussels, A*, no. 318, 1–340.
- Nicolet, M. and Kennes, R. (1986) Aeronomic problems of the molecular oxygen photodissociation—I. The  $O_2$  Herzberg continuum. *Planet. Space Sci.* **34**, 1043.
- Nicolet, M. and Kennes, R. (1988) Aeronomic problems of molecular oxygen photo-dissociation—IV. The various parameters for the Herzberg continuum. *Planet. Space Sci.* **36**, 1069.
- Yoshino, K., Freeman, D. E., Esmond, J. R. and Parkinson, W. H. (1983) High resolution absorption cross section measurements and band oscillator strengths of the (1,0)–(12,0) Schumann–Runge bands of  $O_2$ . *Planet. Space Sci.* **31**, 339.
- Yoshino, K., Freeman, D. E., Esmond, J. R. and Parkinson, W. H. (1987) High resolution absorption cross-sections and band oscillator strengths of the Schumann–Runge bands of oxygen at 79 K. *Planet. Space Sci.* **35**, 1067.
- Yoshino, K., Freeman, D. E. and Parkinson, W. H. (1984) Atlas of the Schumann–Runge absorption bands of  $O_2$  in the wavelength region 175–205 nm. *J. phys. Chem. Ref. Data* **13**, 207.